Journal of the Serbian Chemical Society
JSCS-info@shd.org.rs • www.shd.org.rs/JSCS
J. Serb. Chem. Soc. *83* (12) 1351–1362 (2018)
JSCS–5156
UDC 546.46–31+546.175:548.3:543.55+
621.397.3+544.6.076.32–38
Original scientific paper

Formation of the honeycomb-like MgO/$Mg(OH)_2$ structures with controlled shape and size of holes by molten salt electrolysis

NATAŠA M. VUKIĆEVIĆ[1#], VESNA S. CVETKOVIĆ[1#], NEBOJŠA D. NIKOLIĆ[1]*[#], GORAN BRANKOVIĆ[2], TANJA S. BARUDŽIJA[3] and JOVAN N. JOVIĆEVIĆ[1]

[1]*ICTM – Department of Electrochemistry, University of Belgrade, Njegoševa 12, P. O. Box 473, Belgrade, Serbia,* [2]*Institute for Multidisciplinary Research, University of Belgrade, Kneza Višeslava 1a, Belgrade, Serbia and* [3]*Institute for Nuclear Sciences Vinča, University of Belgrade, P. O. Box 522, 11001 Belgrade, Serbia*

(Received 13 September; revised 4 October, accepted 8 October 2018)

Abstract: Synthesis of the honeycomb-like MgO/$Mg(OH)_2$ structures, with controlled shape and size of holes, by the electrolysis from magnesium nitrate hexahydrate melt onto glassy carbon is presented. The honeycomb-like structures were made up of holes, formed from detached hydrogen bubbles, surrounded by walls, built up of thin intertwined needles. For the first time, it was shown that the honeycomb-like structures can be obtained by molten salt electrolysis and not exclusively by electrolysis from aqueous electrolytes. Analogies with the processes of the honeycomb-like metal structures formation from aqueous electrolytes are presented and discussed. Rules established for the formation of these structures from aqueous electrolytes, such as the increase of number of holes, the decrease of holes size and coalescence of neighbouring hydrogen bubbles observed with increasing cathodic potential, appeared to be valid for the electrolysis of the molten salt used.

Keywords: electrolysis; magnesium nitrate melt; honeycomb-like structure; hydrogen evolution; scanning electron microscope (SEM).

INTRODUCTION

It is known that an electrochemical deposition process can produce nanostructured deposits in controlled manner. Magnesium oxide/hydroxide synthesis by the electrolysis from magnesium nitrate, sulphate and chloride aqueous electrolytes (with different additives and precursors) has been reported.[1–6] However, the additional annealing of electrochemically produced magnesium hydroxide is needed to produce MgO. The additional thermal treatment causes calcination and certain level of magnesium oxide crystallization.[4] We successfully

* Corresponding author. E-mail: nnikolic@ihtm.bg.ac.rs
[#] Serbian Chemical Society member.
https://doi.org/10.2298/JSC180913084V

deposited magnesium oxide/hydroxide on glassy carbon by the electrolysis of magnesium nitrate melt and a variety of morphological forms of deposits were recorded (needle-like, flower-like and honeycomb-like).[7–10] It was found that the current density controlled electrolysis favoured needle-like and flower-like deposit forms and the potential controlled electrolysis favoured flower-like and honeycomb-like structures.

The formation of the honeycomb-like or the 3D (three dimensional) foam structures is of high scientific and technological importance, owing to their possible application as electrodes in many electrochemical devices, such as batteries, sensors and fuel cells, as well as in catalysis.[11–15] Formation of such metal deposits by electrolysis is known as the gas bubble dynamic template or dynamic hydrogen bubble template (DHBT) method. The method implies that the hydrogen bubbles are generated on a working cathode surface, acting as a dynamic template, around which simultaneous electrodeposition of a metal takes place.[11,13,14] Majority of technologically important metals, such as copper,[11,16–18] nickel,[19] silver,[20,21] gold,[22,23] lead[24] and platinum,[25] can be electrochemically deposited from aqueous electrolytes as honeycomb-like or 3D foam structures.

In our resent study[8,10] on magnesium nitrate hexahydrate melt electrolysis, it was reported that some of the magnesium hydroxide/magnesium oxide mixture deposits obtained on glassy carbon, exhibit dish-like holes and the holes constructing a honeycomb-like structures. These closely resemble the typical forms characteristic of electrodeposition of copper in the hydrogen co-deposition range.[12,13,16,26] Considering the high technological significance of the honeycomb-like structures, we continue our investigation with the aim to define the conditions necessary for the controlled synthesis of the honeycomb-like $MgO/Mg(OH)_2$ mixture structure by electrolysis of magnesium nitrate molten salt.

EXPERIMENTAL

A classical three electrode electrochemical system composed of a glassy carbon (GC, Alfa Aeser-Johnson Mathey. Co, USA) working electrode (cathode area approximately 1 cm^2 exposed to the melt), a reference electrode of Mg wire (3 mm in diameter, 99.999%, Luoyang Magnesium Gurnee Metal Material Company. Ltd, Henan, China) and a Mg counter electrode (surface area 7.5 cm^2, 99.999%) was used for electrochemical experiments. The working electrode polished with alumina powder was ultrasonically cleaned in ethanol and deionized water and then dried at room temperature. Magnesium reference and counter electrodes were prepared and cleaned as described earlier.[27-29] Magnesium nitrate hexahydrate ($Mg(NO_3)_2 \cdot 6H_2O$, J.T. Baker, The Netherlands) analytical grade, was used as received and carefully heated under argon stream to the temperature of 373 K.

The working electrode potential was presented *vs.* Mg/Mg^{2+} in the melt used. A potentiostat/galvanostat (EG&G PAR 273A, controlled by Power Suite software, Princeton Applied Research, USA) was used for the electrochemical operations such as cyclic voltammetry (CV) and chronoamperometry.

In contrast to the experimental conditions applied in our earlier work,[8,10] in linear sweep voltammetry experiments (LSV), the potential was swept from starting potential, E_S, being 0.000 V to a final cathodic potential, E_C, of –1.000 V *vs.* Mg/Mg^{2+}, and back to E_S. Experiments under the potentiostatic regime were carried out at: –0.200 V *vs.* Mg/Mg^{2+}, –0.700 V *vs.* Mg/Mg^{2+} and –1.000 V *vs.* Mg/Mg^{2+} applied to the working electrode at T = 373 K. Also, in all electrodeposition processes, the deposition charges were limited to 2 C. After electrolysis, the working electrode was taken out from the cell, rinsed with absolute ethanol (Zorka-Pharma, Šabac, Serbia) and dried at room temperature.

The surface morphology and composition of the deposited samples were characterized by SEM (TESCAN digital microscope; model VEGA3, Brno, Czech Republic) equipped with an energy dispersive spectrometer (EDS). Crystal structure of the deposit obtained by deposition at –0.200 V *vs.* Mg/Mg^{2+} with charge limited to 2C was analysed by Philips PW 1050 powder diffractometer, at room temperature with Ni-filtered CuK$_\alpha$ radiation (λ = 1.54178 Å) and scintillation detector within 2θ 20–75° range in steps of 0.05°, and scanning time of 4 s per step.

RESULTS AND DISCUSSION

Glassy carbon (GC) reversible potential measured in the melt used under experimental conditions was 1.400±0.050 V *vs.* Mg/Mg^{2+}. An example of a cyclic voltammogram recorded with glassy carbon working electrode in the melt used, scanning the potential range from 0.000 V to –1.000 V *vs.* Mg/Mg^{2+} and back, is shown in Fig. 1. There are two well defined broad current waves in the cathodic part of the voltammogram and no anodic counterparts.

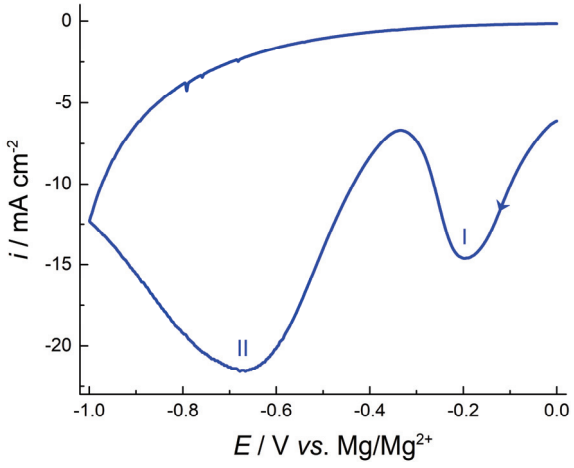

Fig. 1. Cyclic voltammogram of GC in the magnesium nitrate melt; scan rate 10 mV s^{-1} at 373 K.

The first cathodic current wave (I) was observed with the maximum at –0.200 V *vs.* Mg/Mg^{2+} followed by a subsequent drop to the minimum at –0.330 V *vs.* Mg/Mg^{2+}. The second cathodic current maximum (II) was observed at -0.700 V *vs.* Mg/Mg^{2+} and it was followed by a constant current decrease to a minimum at –1.000 V *vs.* Mg/Mg^{2+}. In the anodic scan, there were no current waves which would indicate the oxidation complementary to the two cathodic

current waves. These recordings were in a very good agreement with our previous results, obtained on GC electrode in the same melt[7–10] where starting potential has been E_s = 1.400 V *vs.* Mg/Mg^{2+}.

The most important electrochemical and chemical reactions, from the greater series of 13 reported elsewhere,[10,27,30] responsible for formation of the shown structures can be summarized as:[4,6,10,30,31]

$$2H_2O + 2e^- \rightarrow 2OH^- + H_2 \quad (1)$$

$$Mg^{2+}\cdot + 2H_2O + 2e^- \leftrightarrows Mg(OH)_2 + H_2 \quad (2)$$

$$NO_3^- + H_2O + 2e^- \leftrightarrows NO_2^- + 2OH^- \quad (3)$$

$$NO_3^- + e^- \leftrightarrows NO_2 + O^{2-} \quad (4)$$

$$Mg^{2+}\cdot + 2OH^- \rightarrow Mg(OH)_2 \quad (5)$$

$$Mg^{2+}\cdot + O^{2-} \rightarrow MgO \quad (6)$$

Therefore, the wave I, in Fig. 1, includes the currents reflecting more pronounced reactions given by Eqs. (1) and (3), and wave II recorded the currents reflecting reactions given by Eqs. (1), (2) and (4). The synthesis of magnesium oxide and magnesium hydroxide from the products of the reactions cited here, Eqs. (2), (5) and (6), and elsewhere,[6,10,27,29–31] proceeds at the working electrode surface within the whole potential range applied. Hydrogen gas bubbles produced on the electrode surface and their detachment from the surface provide a fresh area for the electrochemical reactions. However, the gas bubbles do not detach from the electrode surface so easily. Very often, they are detained by very fast growing needle-like and similar $MgO/Mg(OH)_2$ deposit structures which surround and sometimes even cover them.

The chronoamperogram reflecting electrodeposition with restricted charge used at –0.200 V *vs.* Mg/Mg^{2+} is shown in Fig. 2. Typical current–time transient during deposition showed that after about 2500 s cathodic current density decreases down to –0.2 mA cm^{-2}. However, with increasing deposition time the

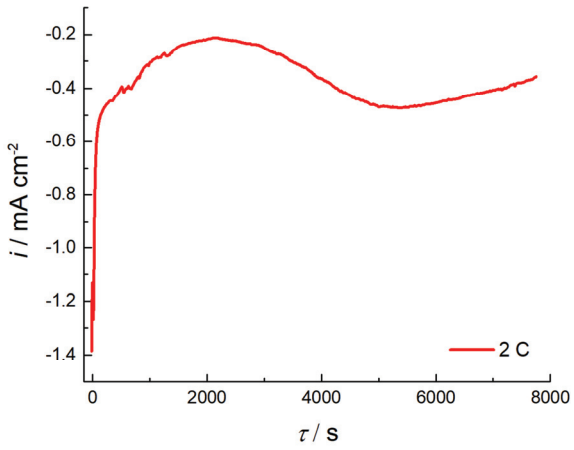

Fig. 2. Current density–time transient recorded on GC electrode from the magnesium nitrate melt used; the potential applied –0.200 V *vs.* Mg/Mg^{2+}; the amount of total charge passed during the deposition restricted to 2 C at 373 K.

current density increased again and reached the maximum of -0.5 mA cm^{-2} at about 5000 s. This maximum is than followed by another slow decrease.

The rise and fall of the current density observed during deposition at -0.200 V *vs.* Mg/Mg^{2+}, using the amount of total charge passed during the deposition restricted to 2 C (Fig. 2), should therefore be attributed to the increase of hydrogen evolution, magnesium cations and nitrate reduction rates on the freed electrode surface (gas bubbles leaving) and the subsequent fall of these rates due to a pseudo-passivation of the electrode surface (Mg oxides and hydroxides being formed).[29,32]

X-ray analysis of the deposit synthesized under potentiostatic regime with 2.0 C applied charge is shown in Fig. 3. XRD pattern revealed that the deposit is composed of a mixture of magnesium hydroxide ($Mg(OH)_2$) and magnesium oxide (MgO). 2θ peaks recorded at 32.8, 50.8, 58.5 and 71.9° should be ascribed to hexagonal $Mg(OH)_2$ (JCPDS No. 01-082-2453). Broader 2θ peak recorded at around 38° and the peak at 62.0° can be ascribed to both MgO and $Mg(OH)_2$ (JCPDS No. 01-075-1525, JCPDS No. 01-082-2453). 2θ peak recorded at 43.1° belongs to MgO periclase (JCPDS No. 01-075-1525).

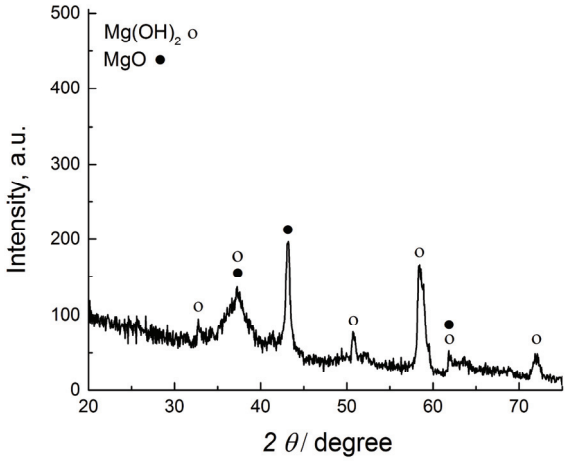

Fig. 3. X-ray diffraction pattern of the electrochemically produced $MgO/Mg(OH)_2$ deposit on GC working electrode from magnesium nitrate melt at potential of –0.200 V *vs.* Mg/Mg^{2+} at 373 K, with charge limited to 2 C.

SEM photographs of the deposits obtained by electrolysis of magnesium nitrate hexahydrate melt used, at working electrode potentials of –0.200, -0.700 and –1.000 V *vs.* Mg/Mg^{2+} using 2.0 C of charge are shown in Figs. 4–6, respectively. The potentials for electrodeposition were selected by the analysis of Fig. 1 and they corresponded to the current waves I and II. Figs. 4–6 revealed that $MgO/Mg(OH)_2$ mixture deposits of honeycomb-like structures have been formed at all three potentials applied.

Fig. 4 shows the honeycomb-like structure obtained at a potential of -0.200 V *vs.* Mg/Mg^{2+}. From Fig. 4a and b, it can be seen that formed honeycomb-like

structure showed regularly distributed holes, made by the detached hydrogen bubbles.

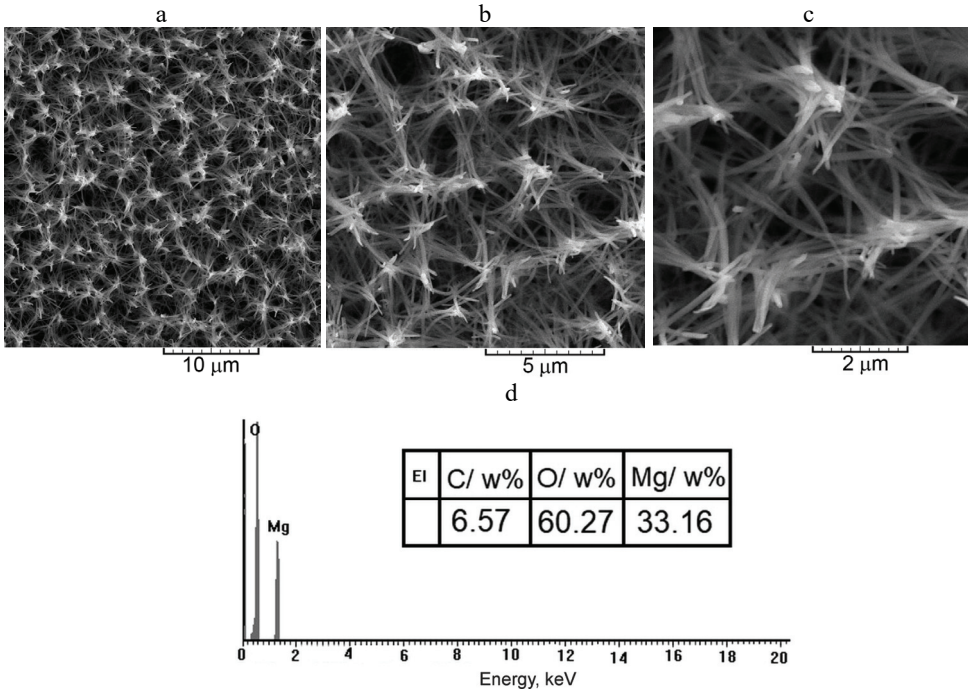

Fig. 4. The honeycomb-like structure obtained on GC electrode from magnesium nitrate hexahydrate melt at the potential of –0.200 V *vs.* Mg/Mg^{2+}; charge applied was 2 C at 373 K; magnifications: a) 4000×; b) 10000×; c) 20000×; d) EDS analysis performed at magnification shown as c.

The average size of the holes recorded was estimated to be around 2 μm (Fig. 4c). It should be noted that the holes were surrounded by very thin nano--sized needles oriented in all directions. Tips of the needles were grouped in bundles making relatively compact wall structure around the holes. The deposit obtained at –0.200 V *vs.* Mg/Mg^{2+} was analysed by EDS and the chemical composition of the honeycomb-like structure is shown in the Fig. 4d.

Figure 5 shows the honeycomb-like structure obtained at the potential of -0.700 V *vs.* Mg/Mg^{2+}, using the same quantity of charge as in Fig. 4. The estimated average hole size was around 1 μm (Fig. 5c). The difference in structural characteristics between deposits in Figs. 4 and 5 was immediately apparent. The increase in the number of holes formed by the detachment of hydrogen bubbles and the decrease of hole sizes has to be attributed to the electrodeposition potential applied (Fig. 5a and b). As expected, the changes in structural characteristics of the obtained honeycomb-like structures can be ascribed to the inten-

sification of hydrogen evolution with the increasing cathodic potential. The increase of the magnesium overpotential applied led to the formation of thinner needles that were highly intertwined around holes.

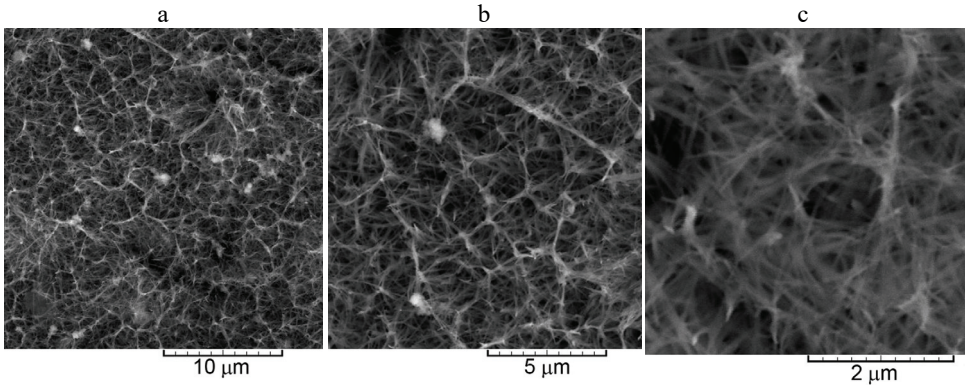

Fig. 5. The honeycomb-like structure obtained on GC electrode from magnesium nitrate hexahydrate melt at the potential of –0.700 V *vs.* Mg/Mg^{2+}; magnifications: a) 5000×; b) 10000×; c) 30000×; charge applied was 2 C at 373 K.

Further increase in the cathodic potential applied led to further intensification of the hydrogen evolution. As a result of vigorous hydrogen evolution and high electrocrystallization rate at the potential of –1.000 V *vs.* Mg/Mg^{2+}, the honeycomb-like structure lost its recognizable regular appearance, as shown in Fig. 6. A number of holes remained captured in the interior of the deposit structure (Fig. 6a). It appears that there was coalescence of the closely formed hydrogen bubbles (Fig. 6b). In the same time there is a portion of needles which mutually coalesced to make a compact surface of this structure type (Fig. 6c).

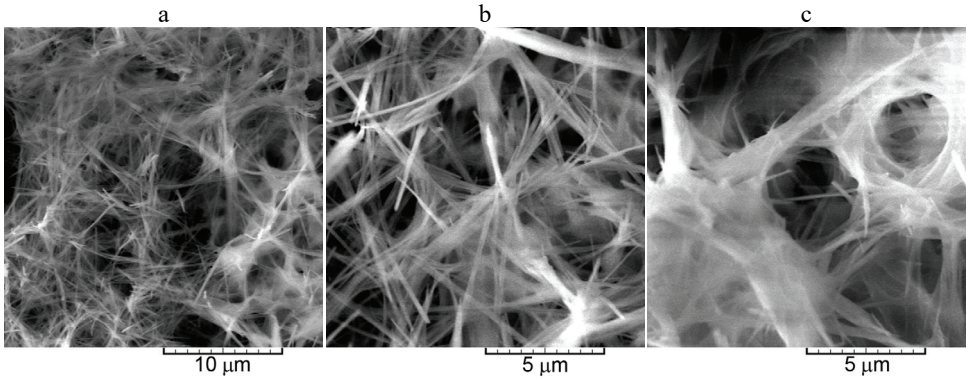

Fig. 6. The honeycomb-like structure obtained on GC electrode from magnesium nitrate hexahydrate melt at the potential of –1.000 V *vs.* Mg/Mg^{2+}; magnifications: a) 5000×; b) 10000×; c) 10000×; charge applied was 2.0 C at 373 K.

Hence, unlike the results presented in our previous reports,[7–10] where the flower-like forms, as well as a mixture of dish-like holes and holes constructing the honeycomb-like structure were obtained, here we show that it is possible to define conditions that enable a formation of the uniform honeycomb-like structures of the controlled shape and size of the holes formed from the detached hydrogen bubbles. It is attained by the careful selection of electrolysis conditions. Namely, in our recent investigation,[10] the pulse of 1.400 V *vs.* Mg/Mg^{2+} preceded to the electrolysis at the selected potential, by which the flower-like forms and dish-like holes were formed. The absence of this pulse enabled formation of uniform honeycomb-like structures. Anyway, the analysis of the honeycomb-like structures presented in Figs. 4–6 showed that the honeycomb-like structure obtained at –0.200 V *vs*. Mg/Mg^{2+} was more uniform than those formed at potentials of –0.700 and –1.000 V *vs.* Mg/Mg^{2+}. This can be ascribed to the fact that the increase in cathodic potential causes both intensification of the hydrogen evolution reaction and the increase of the magnesium oxide/magnesium hydroxide electrocrystallization rate.

From the presented results, it is apparent that the honeycomb-like structures can be synthetized not only by the electrolysis from aqueous electrolytes, but also by the electrolysis from melt, as shown in this work. Additionally, it appears that similar rules are valid for the formation of honeycomb-like structures made of metals being deposited from aqueous electrolytes and honeycomb-like structures made of $MgO/Mg(OH)_2$ mixtures, being obtained by the electrolysis of magnesium nitrate melt. The rules seem to be determined by the increase of number of holes originating from the detached hydrogen bubbles, by the decrease of their size, and by coalescence of neighbouring bubbles, as a result of an intensification of hydrogen evolution reaction with the increasing cathodic potential.[11–15] Therefore, it seems logical to discuss the analogies between the formations of honeycomb-like metal structures obtained by the electrolysis from the aqueous electrolytes and the formation of honeycomb-like $MgO/Mg(OH)_2$ structures obtained by the electrolysis of the magnesium nitrate hexahydrate melt.

According to Winand,[33] in the dependence of the exchange current density, melting points and overpotentials for hydrogen discharge, metals are classified into three groups: normal, intermediate and inert ones. The group of the normal metals, such as Pb, Sn, Ag, Cd and Zn, is characterized by the high values of both the exchange current density and overpotential for hydrogen evolution, as well as by the low melting points. The group of the intermediate metals, such as Cu, Au and Ag (ammonium electrolyte) is characterized by the lower values of the exchange current density and overpotential for hydrogen evolution than the normal metals. Finaly, the third group of metals makes the so-called the inert metals, such as Ni, Co, Pt and Pd, and they are characterized by both low

exchange current densities and overpotentials for hydrogen evolution, as well as by the high melting points.

The fact that well defined needles oriented in all directions were formed among holes, indicates that $MgO/Mg(OH)_2$ mixture behaves almost as the normal metal. One of the main characteristics of electrodeposition of the normal metals is diffusion control starting from very low potentials[13,34] as confirmed here by the formation of well defined needles in a whole range of examined potentials. For comparison, the needle-like, as well as the other type of dendritic forms, are also formed starting from low cathodic potentials during electrodeposition processes of Pb and Ag (the typical representatives of the normal metals) from the aqueous electrolytes.[13] On the other hand, the $MgO/Mg(OH)_2$ mixture shows certain characteristics that define the so-called inert metals. Low values of both the exchange current density and the overpotential for hydrogen evolution reaction means that there is a parallel between metal electrodeposition process and the hydrogen evolution reaction in the whole range of potentials.[13,35] In this case, the honeycomb-like structures are formed throughout the magnesium OPD region. However, the fact that well defined needles similar to those formed around holes are obtained in the magnesium UPD region where there is no hydrogen evolution,[10] suggests that the formation of the $MgO/Mg(OH)_2$ deposit still behaves as the normal metal. This implies that the evolved hydrogen had no effect on the hydrodynamic conditions in the near-electrode layer, and hence, on the morphology of the deposits around the holes. The similar situation is observed during the formation of the honeycomb-like structure of Pb, as one of the most important representatives from the group of the normal metals.[24] The very thin needles were formed around the holes during electrodeposition of Pb in the honeycomb-like form.

CONCLUSION

The processes of electrolysis from magnesium nitrate hexahydrate melt have been analyzed by the linear sweep voltammetry (LSV) and chronoamperometry, while morphology of the deposits obtained by the potentiostatic regime of electrolysis was characterized by the techniques of scanning electron microscopy (SEM) and EDS. The XRD analysis of the deposit showed that $MgO/Mg(OH)_2$ mixture was obtained by this electrolysis process.

It was shown that the honeycomb-like structures made of $MgO/Mg(OH)_2$ mixture constructed around the holes originating from the detached hydrogen bubbles and surrounded by the thin intertwined needles were formed in a wide range of cathodic potentials applied. The shape and the size of holes were strongly controlled by the choice of the cathodic potential.

All factors influencing the formation of the honeycomb-like metal structures obtained by the electrolysis from aqueous electrolytes appeared to govern the

formation of the honeycomb-like $MgO/Mg(OH)_2$ structures, obtained from the molten salt electrolysis onto glassy carbon working electrode. This analogy with the formation of the honeycomb-like metal structures from the aqueous electrolytes suggested that, in spite of the vigorous hydrogen evolution, $MgO/Mg(OH)_2$ deposit formation behaved as a deposit characteristic for electrodeposition of the normal metal.

Acknowledgement. The work was supported by the Ministry of Education, Science and Technological Development of the Republic of Serbia (Grants No. 172046 and 172060).

ИЗВОД

ФОРМИРАЊЕ $MgO/Mg(OH)_2$ СТРУКТУРА НАЛИК ПЧЕЛИЊЕМ САЋУ КОНТРОЛИСАНОГ ОБЛИКА И ВЕЛИЧИНЕ РУПА ЕЛЕКТРОЛИЗОМ ИЗ РАСТОПА

НАТАША М. ВУКИЋЕВИЋ[1], ВЕСНА С. ЦВЕТКОВИЋ[1], НЕБОЈША Д. НИКОЛИЋ[1], ГОРАН БРАНКОВИЋ[2], ТАЊА С. БАРУЦИЈА[3] и ЈОВАН Н. ЈОВИЋЕВИЋ[1]

[1]ИХТМ – Центар за електрохемију, Универзитет у Београду, Његошева 12, Београд, [2]Институт за мултидисциплинарна истраживања, Универзитет у Београду, Кнеза Вишеслава 1а, Београд и [3]Институт за нуклеарне науке Винча, Универзитет у Београду, п. пр. 522, 11001 Београд

Представљено је формирање $MgO/Mg(OH)_2$ структура облика пчелињег саћа контролисаног облика и величине рупа, процесом електролизе растопљеног магнезијум-нитрата-хексахидрата на стакластом угљенику. Добијене структуре пчелињег саћа су се састојале од рупа, формираних одвајањем мехурова водоника, окружених зидом од танких испреплетаних игала. По први пут је показано да се структуре пчелињег саћа могу добити не само електролизом из водених електролита, већ такође и електролизом из растопа. Аналогије са процесима формирања талога облика пчелињег саћа из водених раствора су изнесене и продискутоване. Све законитости утврђене за формирање ових структура из водених електролита, као што су повећање броја рупа, смањење величине рупа и сједињавање суседних мехурова водоника посматраних са повећањем катодног потенцијала, важе и за електролизу из растопа.

(Примљено 13. септембра, ревидирано 4. октобра, прихваћено 8. октобра 2018)

REFERENCES

1. Y. Ding, G. Zhang, H. Wu, B. Hai, L. Wang, Y. Qian, *Chem. Mater.* **13** (2001) 435 (http://dx.doi.org/10.1021/cm000607e)
2. N. M. Julkapli, S. Bagheri, *Rev. Inorg. Chem.* **36** (2016) 1 (http://dx.doi.org/10.1515/revic-2015-0010)
3. G. Zou, R. Liu, W. Chen, *Mater. Lett.* **61** (2007) 1990 (http://dx.doi.org/10.1016/j.matlet.2006.07.172)
4. G. Zou, W. Chen, R. Liu, Z. Xu, *Mater. Chem. Phys.* **107** (2008) 85 (http://dx.doi.org/10.1016/j.matchemphys.2007.06.046)
5. M. Dinamani, P. V. Kamath, *J. Appl. Electrochem.* **34** (2004) 899 (http://dx.doi.org/10.1023/B:JACH.0000040437.81319.56)
6. C.-F. Li, W.-H. Ho, S.-K. Yen, *J. Electrochem. Soc.* **156** (2009) E29 (http://dx.doi.org/10.1149/1.3032174)
7. V. S. Cvetković, N. Jovićević, J. N. Jovićević, in *Proceedings of 62th Annual Meeting Int. Soc. Electrochem.*, ISE, Niigata, Japan, 2011, pp. s03–P-013
8. V. S. Cvetković, N. M. Vukićević, N. D. Nikolić, G. Branković, J. N. Jovićević, in *Proceedings of XIX YuCorr Int. Conf.*, Tara, Serbia, 2017, p. 183

9. V. Cvetković, N. Vukićević, J. Stevanović, J. Jovićević, in *Proceedings of 48th Int. Oct. Conf.*, TF, Bor, Serbia, 2016, pp. 301–305
10. V. S. Cvetković, N. M. Vukićević, N. D. Nikolić, G. Branković, T. S. Barudžija, J. N. Jovićević, *Electrochim. Acta* **268** (2018) 494 (http://dx.doi.org/10.1016/j.electacta.2018.02.121)
11. H.-C. Shin, J. Dong, M. Liu, *Adv. Mater.* **15** (2003) 1610 (http://dx.doi.org/10.1002/adma.200305160)
12. N. D. Nikolić, in *Electrochem. Prod. Met. Powders, Ser. Mod. Asp. Electrochem.*, S. S. Djokić (Ed.), Springer, New York, 2012, pp. 187–249 (ISBN 978-1-4614-2380-5)
13. K. I. Popov, S. S. Djokić, N. D. Nikolić, V. D. Jović, *Morphology of Electrochemically and Chemically Deposited Metals*, Springer International Publishing, New York, 2016 (ISBN 978-3-319-26073-0)
14. B. J. Plowman, L. A. Jones, S. K. Bhargava, *Chem. Commun.* **51** (2015) 4331 (http://dx.doi.org/10.1039/C4CC06638C)
15. M. Wang, X. Yu, Z. Wang, X. Gong, Z. Guo, L. Dai, *J. Mater. Chem., A* **5** (2017) 9488 (http://dx.doi.org/10.1039/C7TA02519J)
16. N. D. Nikolić, K. I. Popov, Lj. J. Pavlović, M. G. Pavlović, *J. Electroanal. Chem.* **588** (2006) 88 (http://dx.doi.org/10.1016/j.jelechem.2005.12.006)
17. N. Nikolić, Lj. Pavlović, G. Branković, M. Pavlović, K. Popov, *J. Serb. Chem. Soc.* **73** (2008) 753 (http://dx.doi.org/10.2298/JSC0807753N)
18. H. Zhang, Y. Ye, R. Shen, C. Ru, Y. Hu, *J. Electrochem. Soc.* **160** (2013) D441 (http://dx.doi.org/10.1149/2.019310jes)
19. X. Yu, M. Wang, Z. Wang, X. Gong, Z. Guo, *Appl. Surf. Sci.* **360** (2016) 502 (http://dx.doi.org/10.1016/j.apsusc.2015.10.174)
20. S. Cherevko, C.-H. Chung, *Electrochim. Acta* **55** (2010) 6383 (http://dx.doi.org/10.1016/j.electacta.2010.06.054)
21. S. Cherevko, X. Xing, C.-H. Chung, *Electrochem. Commun.* **12** (2010) 467 (http://dx.doi.org/10.1016/j.elecom.2010.01.021)
22. S. Cherevko, C.-H. Chung, *Electrochem. Commun.* **13** (2011) 16 (http://dx.doi.org/10.1016/j.elecom.2010.11.001)
23. B. J. Plowman, A. P. O'Mullane, P. Selvakannan, S. K. Bhargava, *Chem. Commun.* **46** (2010) 9182 (http://dx.doi.org/10.1039/c0cc03696j)
24. S. Cherevko, X. Xing, C.-H. Chung, *Appl. Surf. Sci.* **257** (2011) 8054 (http://dx.doi.org/10.1016/j.apsusc.2011.04.098)
25. A. Ott, L. A. Jones, S. K. Bhargava, *Electrochem. Commun.* **13** (2011) 1248 (http://dx.doi.org/10.1016/j.elecom.2011.08.032)
26. N. D. Nikolić, L. J. Pavlović, M. G. Pavlović, K. I. Popov, *Electrochim. Acta* **52** (2007) 8096 (http://dx.doi.org/10.1016/j.electacta.2007.07.008)
27. V. S. Cvetković, L. J. Bjelica, N. M. Vukićević, J. N. Jovićević, *Chem. Ind. Chem. Eng. Q.* **21** (2015) 527 (http://dx.doi.org/10.2298/CICEQ141205009C)
28. V. S. Cvetković, J. N. Jovićević, L. J. Bjelica, *Kov. Mater.* **54** (2016) 321 (http://dx.doi.org/10.4149/km_2016_5_1)
29. V. S. Cvetković, N. Jovićević, J. S. Stevanović, M. G. Pavlović, N. M. Vukićević, Z. Stevanović, J. N. Jovićević, *Metals* **7** (2017) (http://dx.doi.org/10.3390/met7030095)
30. D. A. Tkalenko, *Electrokhimiya Nitratnykh Rasplavov*, Naukova Dumka, Kiev, Ukraine, 1983
31. R. Hashaikeh, J. A. Szpunar, *J. Phys. Conf. Ser.* **165** (2009) 012008 (http://dx.doi.org/10.1088/1742-6596/165/1/012008)

32. J. E. Vindstad, H. Mediaas, T. Østvold, L. Skattebøl, C. N. Rosendahl, *Acta Chem. Scand.* **51** (1997) 1192 (http://dx.doi.org/10.3891/acta.chem.scand.51-1192)
33. R. Winand, *Electrochim. Acta* **39** (1994) 1091 (http://dx.doi.org/10.1016/0013-4686(94)E0023-S)
34. N. Nikolić, P. Zivković, G. Branković, M. Pavlović, *J. Serb. Chem. Soc.* **82** (2017) 539 (http://dx.doi.org/10.2298/JSC161114029N)
35. V. Maksimović, N. Nikolić, V. Kusigerski, J. Blanuša, *J. Serb. Chem. Soc.* **80** (2015) 197 (http://dx.doi.org/10.2298/JSC200814104M).